Nano Hybrids and Composites
ISSN: 2297-3400, Vol. 44, pp 53-69
doi:10.4028/p-0Qhsjl
© 2024 Trans Tech Publications Ltd, Switzerland
Submitted: 2023-05-09
Revised: 2024-03-24
Accepted: 2024-04-04
Online: 2024-06-26

Hydrothermal Characteristics-Based Water Purification Model Using Hybrid Nanofluid Flow over Non-Linearly Stretched Permeable Surfaces

A.M. Obalalu[1,a*], O.A. Olayemi[2,b], S.A. Salaudeen[3,c], A.D. Adeshola[4,d], O.B. Ojewola[5,e], A.O. Akindele[6,f], O.A. Oladapo[7,g]

[1]Department of Mathematical Sciences, Augustine University Ilara Epe, Lagos, Nigeria,

[2]Department of Aeronautics and Astronautics, Faculty of Engineering and Technology, Kwara State University, Malete, Nigeria.

[3]Department of Physics with Electronics, Faculty of Sciences and Computing, Ahman Pategi University, Patigi.

[4]Department of Mathematics and Statistics, Kwara State University, Malete, Nigeria.

[5,6,7]Department of Mathematics, Ladoke Akintola University of Technology, Ogbomoso, Nigeria.

[a]adebowale.obalalu17@gmail.com, [b]olalekan.olayemi@kwasu.edu.ng,
[c]aoakdelr5@pgschool.lautech.edu.ng, [d]adeshola.daud@kwasu.edu.ng
[e]olusegunbaba9@gmail.com , [f]aoakindele21@lautech.edu.ng, [g]aakeemoladapo1@gmail.com.
[*]Corresponding Authors: adebowale.obalalu17@gmail.com

Keywords: Thermodynamic Irreversibility, hybrid Nanofluid, Iron (III) Oxide, Copper, Galerkin Weighted Residual Method.

Abstract: Sequel to all the published facts on the hydrothermal of pure water on a permeable expanding/contracting surface with thermodynamic irreversibility convey iron (III) oxide and copper hybrid nanoparticles as applicable in industry and engineering, nothing is known about the importance of viscous dissipation and the Joule heating. The current paper addresses the natural convective flow of pure water, Fe_3O_4/H_2O nanofluid and Fe_3O_4-Cu/H_2O hybrid nanofluid, (a novel advanced nanofluid composited of Fe_3O_4 and Cu nanoparticles) induced by a non-linearly stretching permeable sheet with velocity slip using a numerical scheme. The equations obtained are solved numerically via Galerkin Weighted Residual Method (GWRM), in the limiting sense, the present results conform with the existing work. Analyses reveal that a 20% concentration of nanoparticles in a base fluid is more effective in the augmentation of heat transfer than a 10% concentration. Also, the Nonlinearity parameter increased the heat transfer rate for the hybrid nano-suspension. The report of this study will be of benefit to chemical engineering and nanotechnology advancement.

Nomenclature

μ_{hnf}	hybrid nanofluid dynamic viscosity	x	coordinate long the surface
ρ_{hnf}	hybrid nanofluid heat capacity	y	vertical coordinate
σ_{hnf},	hybrid nanofluid electrical conductivity	y, u and v	component of the velocity along x and y directions
k_{hnf}	hybrid nanofluid thermal conductivity	T	hybrid nanofluid temperature
$(\rho C_p)_{hnf}$	hybrid nanofluid density	σ_v	tangential momentum accommodation coefficient
$v_w(x)$	suction (injection) velocity	$\lambda(x)$	mean free path
r	surface temperature parameter	T_w	wall temperature
nf	nanofluid	f	base fluid
n_1 and n_2	hybrid nano particles	$Cu(\varphi_{n_1})$	Nanoparticle volume fraction of the copper
M	magnetic parameter	$Fe_3O_4(\varphi_{n_2})$	Nanoparticle volume fraction of the iron oxide
Pr	Prandtl number	Ec	Eckert number
δ	velocity slip	C_{fx}	skin friction coefficient

All rights reserved. No part of contents of this paper may be reproduced or transmitted in any form or by any means without the written permission of Trans Tech Publications Ltd, www.scientific.net. (#653108162-26/06/24,15:19:18)

Re_x	local Reynolds number	Nu_x	Nusselt number
$S = f(0)$	denotes the constant mass flux parameter	ψ	stream function
$S < 0$	depicts fluid injection	$S > 0$	signifying fluid suction
ν_f	represent the kinematic viscosity of base fluid	Ω	temperature difference parameter

1. Introduction

In the last decade, scientists have been exploring the combining of nanoparticles with different base fluids to improve the thermal conductivity of base fluids including water, kerosene oil, propylene glycol, and ethylene glycol. The resultant fluids have a variety of properties and can be employed in applications including engineering, process industries, biomedical, and cancer therapy, cooling. Maxwell [1] was the first scientist to prove that, a solid-liquid mixture can increase thermal conductivity with higher solid particle volume. However, large particles produce several troubling problems, which including the deposition of the large particles in the base fluid, particularly in low speed, obstruction, pressure decrease, and pipe erosion. Therefore, a new fluid class has been established which is named nanofluid to improve both thermal conductivity and stabilization of suspensions. Nanofluids are a novel type of multicomponent fluids that consist of nanometer-size (metallic or non-metallic) particles that are uniformly disseminated and suspended within a base fluid. Researchers [2-4] conducted experiments that show that a higher rate of heat transmission and thermal conductivity of base fluids at 5%, 10%, and 55% volume fractions of nanoparticles are chosen. However, it was observed that the highest effect of heat transfer rate is shown to be possible at 5% of the volume fraction of nanoparticles. Eastman et al. [5] exhibited that the thermal conductivity enhances by 40% when the 0.3% volume concentration of Cu nanoparticles was disseminated into ethylene glycol.

Water is widely employed in the industry for nanofluid processing since it is easily accessible and affordable. Water is a solvent that can be used in a variety of situations in dissolve of a higher proportion of a substance or nanoparticles to improve the solubility, suspension, or colloidal suspension [6]. Hassan et al. [7] emphasized that the features of water that include low thermal conductivity need to be modified if the water is used by nanoparticles as a heat exchanger. However, water is commonly described as the base fluid because it has a pH of 7 and can only exist in three states in nature. Therefore, the surface tension of water is high and allowed the microscopic particles to circulate across their surface. Consequently, it can be detected within the spectrum as a suitable transportation medium [8]. In addition, Rust is generated by combining iron to produce hydrated iron (III) oxide (III) (Fe_3O_4) with oxygen and water. However, Iron and steel rust when they are contacted to water and oxygen.Also, Iron does not change when exposed to pure water or dry air, but it corrodes when exposed to both water and oxygen (wet air). Therefore (Fe_3O_4-H_2O) Is the chemical formula for rust. It transforms silver color to reddish-brown since it forms hydrated oxides. Iron extraction is usually done in the manufacturing of drinking water since there is a considerable quantity of iron ions in mineral water. Further, copper (Cu) is a versatile base metal that is commonly used to enhance the elasticity, flexibility, hardness, color, and corrosion resistance of precious metals. Cu is among the metals that can be found in large amounts in water. Drinking water preserved in a copper vessel is a safe and good health practice, according to new findings [9].

Devi and Devi [10] exhibited that utilizing copper-alumina/water as convectional fluid improvement of convective heat transfer over a stretched surface. The heat transfer rate of ZnO/H_2O nanofluid flow in a circular tube was investigated by Sajadi et al. [11] , and it was discovered that when the volume fraction of nanoparticles is between 2 and 4 %, the heat transfer rate improves more efficiently. Also, the copper-water nanofluid was examined via Sheikholeslami et al. [12] and conclude that the nanofluid improves the Nusselt number and reduces the pressure. Khan et al. [13] examined the Blasius–Rayleigh–Stokes flow of water-based alumina- iron (III) oxide passing through a semi-finite heated plate. Free vibration analysis of composite material plates" Case of a typical functionally graded FG plates ceramic/metal" with porosities were study by [14]. Investigation on Mechanical,

Thermal and Bonding Properties of MWCNTs Reinforced Aramid/Epoxy composite were study by [15]. Entropy generation on maxwell fluid flow past an inclined stretching plate with slip and convective surface condition: Darcy-forchheimer model were study by [16].

Almost all studies on nanofluids that have been published so far, described the describes Nanofluid as a basis nanofluid containing a single substance kind of suspended nano-sized particles [17]. They explored the impact on the thermophysical characteristic of nanofluid and their effect on the heat transfer rate of size, shape, concentration, and material of nanoparticles dispersed in a fluid. Nevertheless, it was very recently that research into the novel type of operational fluid with double forms of nanoparticles, at the same time dispersed in a base liquid called hybrid nanofluid, was conducted by Suresh et al. [18]. Therefore, further study into the segmented hybrid nanofluid mixtures is necessary to increase the efficiency of heat transfer by mixing their ratios. The major aim of this novel type of nanofluid is to improve the thermophysical characteristics as well as the heat transfer rate, with regard to the practical applications in a variety of technologies such as hybrid-powered engines, solar energy, and biomedical, where such a novel type of nanofluid an effectively be applied [19]. In regards to this, Turcu et al. [20] pioneered the study of characterization and mixtures of nanocomposite hybrid particles. The copper-iron oxide\water of hybrid nanofluid on nonlinearly shrinking/stretching surfaces was studied by [21]. Acharya et al. [22] discussed the significance of magnetic field and slip surfaces on hybrid nanofluid flow. Hayat et al. [15] used the Darcy-Forchheimer porous media model to examine the nonlinear thermal radiation over a stretched surface of a water-based hybrid nanofluid.

In a real-life process, entropy generation clarifies the system stability at molecule. The evolution of the thermodynamics process due to irreversibility can be described in terms of entropy generation[23, 24]. Many researchers are interested in the study of entropy generation since it helps regulate thermal systems' irreversibility losses, which may reduce system efficiency [25]. Entropy generation can be used to characterize the development of the thermodynamics process due to irreversibility. The evolution of the thermodynamics process due to irreversibility can be described in terms of entropy generation. Obalalu et al. [26] investigated the heat transfer enhancement on the thermodynamics process of an unsteady Newtonian fluid with the existence of a convective heating effect. The entropy generation and hydrodynamic slip of hybrid nanofluid with temperature-dependent convection were studied by [27]. A mathematical model namely Optimal Homotopy Analysis Method (OHAM) was established by [28] to study the nanofluid of entropy generation and thermal conductivity of natural convective. Their research revealed that while the rate of entropy creation decreases with an increase in the Maxwell parameter and the inertia coefficient, the rate of entropy formation increases with increases in the porosity parameter and thermal radiation parameter.

In light of the above discussions, the aim of this present exploration based Fe_3O_4- Cu/H_2O hybrid nanofluid and joule heating effect on heat transfer and thermodynamic irreversibility by utilizing Tiwari and Das model [29]. Moreover, iron (III) oxide (Fe_3O_4) and copper (Cu) nanoparticles are suspended in water to generate hybrid composites. The study of thermodynamic Irreversibility is included to explore the flow and heat transfer. Although hybrid nanofluid is rarely studied, none of the papers that have been published in this area have studied in detail how the viscous dissipation, joule heating. magnetic field, and suction/injection along non-linearly stretching permeable sheet with velocity slip using nanofluid Tiwari-Das type influences the entropy generation. To the best of knowledge, no study into the aforementioned problems has yet been published. Results from this study will help scientists to improve the heat transfer rates and thermodynamic irresistibility for hybrid nanofluids.

2. Mathematical Model

A steady two-dimensional laminar flow of non-linearly stretching permeable sheet with velocity slip and prescribed surface heat flux in an electrically conducting viscous hybrid nanofluid is analyzed. A non-uniform magnetic field acts normal to the flow direction with strength $B(x) = B_0 x^{(m-1)/2}$ where B_0 is the applied magnetic field strength. The permeable sheet is stretching with assumed

velocity of $u_w(x) = ax^m$Also, the external velocity takes $u_e = cx^m$ where a and c are positive constant. Here, $m \neq 1$is the nonlinearity parameter.Impending the boundary layer, the prevailing equations corresponding to the hybrid nanofluid and those related to heat transfer are derived in [30]:

$$\frac{\partial u}{\partial x} + \frac{\partial v}{\partial y} = 0 \tag{1}$$

$$u\frac{\partial u}{\partial x} + v\frac{\partial u}{\partial y} = u_e\frac{du_e}{dx} + \frac{\mu_{hnf}}{\rho_{hnf}}\frac{\partial^2 u}{\partial y^2} - \frac{\sigma_{hnf}B(x)^2}{\rho_{hnf}}(u_e - u) \tag{2}$$

$$u\frac{\partial T}{\partial x} + v\frac{\partial T}{\partial y} = \frac{k_{hnf}}{(\rho C_p)_{hnf}}\frac{\partial^2 T}{\partial y^2} + \frac{\mu_{hnf}}{(\rho C_p)_{hnf}}\left(\frac{\partial u}{\partial y}\right)^2 + \frac{\sigma_{hnf}B(x)^2}{(\rho C_p)_{hnf}}(u_e - u)^2. \tag{3}$$

$$S'''_{gen} = \frac{k_{hnf}}{T_\infty^2}\left(\frac{\partial T}{\partial y}\right)^2 + \frac{\mu_{hnf}}{T_\infty}\left(\frac{\partial u}{\partial y}\right)^2 + \frac{\sigma_{hnf}}{T_\infty}B_0^2(x)(u_e - u)^2 \tag{4}$$

Subjected to [13]:

$$\begin{aligned} &u = u_w(x) + \lambda(x)\frac{\mu_{hnf}}{\rho_{hnf}}\frac{\partial u}{\partial y}, \quad v = v_w(x), \quad T = T_w(= T_\infty + Ax^r), \text{at} \quad y = 0, \\ &u \longrightarrow u_e(x), \quad T \longrightarrow T_\infty, \text{as} \quad y \longrightarrow \infty. \end{aligned} \tag{5}$$

Thermo-physical features of simple nanofluid defined as [31, 32]:

$$\left.\begin{aligned} \mu_{nf} &= \frac{\mu_f}{(1-\varphi_{Cu})^{2.5}} \\ k_{nf} &= \frac{k_{Cu}+2k_f-2\varphi_{Cu}(k_f-k_{Cu})}{k_{Cu}+2k_f+\varphi_{Cu}(k_f-k_{Cu})} \times k_f, \\ \sigma_{nf} &= 1 + \frac{3\left(\frac{\sigma_{Cu}}{\sigma_f} - 1\right)\varphi_{Cu}}{2 + \frac{\sigma_{Cu}}{\sigma_f} - \left(\frac{\sigma_{Cu}}{\sigma_f} - 1\right)\varphi_{Cu}} \times \sigma_f, \\ \rho_{nf} &= (1-\varphi_{Cu})\rho_f + \varphi_{Cu}\rho_{Cu}, \\ (\rho C_p)_{nf} &= (1-\varphi_{Cu})(\rho C_p)_f, + \varphi_{Cu}(\rho C_p)_{Cu} \end{aligned}\right\} \tag{6}$$

Thermophysical properties of hybrid nanoparticles are defined as[33]:

$$\left.\begin{aligned} \mu_{hnf} &= \frac{\mu_f}{(1-\varphi_{Cu})^{2.5}(1-\varphi_{Fe_3O_4})^{2.5}} \\ k_{hnf} &= \frac{k_{Fe_3O_4}+2k_{nf}-2\varphi_{Fe_3O_4}(k_{nf}-k_{Fe_3O_4})}{k_{Fe_3O_4}+2k_{nf}+\varphi_{Fe_3O_4}(k_{nf}-k_{Fe_3O_4})} \times k_{nf}, \text{ where } k_{nf} = \frac{k_{Cu}+2k_f-2\varphi_{Cu}(k_f-k_{Cu})}{k_{Cu}+2k_f+\varphi_{Cu}(k_f-k_{Cu})} \times k_f \\ \sigma_{hnf} &= \frac{\sigma_{Fe_3O_4}+2\sigma_{nf}-2\varphi_{Fe_3O_4}(\sigma_{nf}-\sigma_{Fe_3O_4})}{\sigma_{Fe_3O_4}+2\sigma_{nf}+\varphi_{Fe_3O_4}(\sigma_{nf}-\sigma_{Fe_3O_4})} \times \sigma_{nf}, \ \sigma_{nf} = \frac{\sigma_{Cu}+2\sigma_f-2\varphi_{Cu}(\sigma_f-\sigma_{Cu})}{\sigma_{Cu}+2\sigma_f+\varphi_{Cu}(\sigma_f-\sigma_{Cu})} \times \sigma_f \\ \rho_{hnf} &= (1-\varphi_{Fe_3O_4})\left[(1-\varphi_{Cu})\rho_f + \varphi_{Cu}\rho_{n_1}\right] + \varphi_{Fe_3O_4}\rho_{Fe_3O_4} \\ (\rho C_p)_{hnf} &= (1-\varphi_{Fe_3O_4})\left[(1-\varphi_{Cu})(\rho C_p)_f + \varphi_{Cu}(\rho C_p)_{n_1}\right] \varphi_{Fe_3O_4}(\rho C_p)_{Fe_3O_4} \end{aligned}\right\} \tag{7}$$

Table 1display physical characteristics of the base fluid and hybrid nanofluid [13, 34, 35].

Table 1. The physical characteristics of the base fluid and hybrid nanofluid

Physical property	Water (H_2O)	Iron oxide (Fe_3O_4)	Copper (Cu)
$\rho/(kg.m^{-3})$	997.1	5180	8933
$k/(W.mK)$	0.613	8.9528	400
$C_p/(J.kgK)$	4 179	670	385
$\sigma/(S.m)$	0.5×10^{-6}	0.7×10^{-6}	5.96×10^{7}

The mathematical representations used in the model are explicitly described in the nomenclature. The following Stream functions with similarity variables were introduced:

$$\left.\begin{gathered} u=\frac{\partial\psi}{\partial y}\text{and } v=-\frac{\partial\psi}{\partial x} \\ \eta=\left(\frac{a}{\nu_f}\right)^{\frac{1}{2}}x^{\frac{m+1}{2}}y,\psi=(a\nu_f)^{1/2}x^{(m+1)/2}f(\eta),\theta(\eta)=\frac{T-T_\infty}{T_w-T_\infty}, \end{gathered}\right\} \tag{8}$$

By substituting (5)) and (4) into Eq. (1)-(4), the similarity equations are as follows:

$$\frac{A_1}{A_2}f'''+\frac{m+1}{2}ff''+m(1-f'^2)-\frac{A_3}{A_2}M(f'-1)=0, \tag{9}$$

$$\frac{1}{Pr}\frac{A_4}{A_5}\theta''+\frac{(m+1)}{2}f\theta'-2mf'\theta+\frac{Ec}{A_5}[A_1f''^2+A_3M(1-f')^2]=0, \tag{10}$$

$$Ns=A_4\theta'^2+\frac{EcPr}{\Omega}[A_1f''^2+A_3M(1-f')^2] \tag{11}$$

subjected to:

$$\begin{gathered} f(0)=S,\quad f'(0)=\varepsilon+\delta\frac{A_1}{A_2}f''(0),\quad \theta(0)=1, \\ f'(\eta)\longrightarrow 1,\quad \theta(\eta)\longrightarrow 0\text{as}\quad \eta\longrightarrow\infty, \end{gathered} \tag{12}$$

The Bejan number (Be) is defined as

$$Be=\frac{A_4\theta'^2}{A_4\theta'^2+\frac{EcPr}{\Omega}[A_1f''^2+A_3M(1-f')^2]}, \tag{13}$$

where

$$\left.\begin{gathered} A_2=\frac{\rho_{hnf}}{\rho_f},A_3=\frac{\sigma_{hnf}}{\sigma_f},A_4=\frac{k_{hnf}}{k_f},A_5=\frac{(\rho C_p)_{hnf}}{(\rho C_p)_f} \\ \tau_w(x)=\mu_{hnf}(\partial u/\partial y)_{y=0},q_w(x)=-k_{hnf}(\partial T/\partial y)_{y=0},Re_x=\frac{u_e x}{\nu_f}. \\ v_w(x)=-\frac{(a\nu_f)^{1/2}(m+1)}{2}x^{(m-1)/2}S\quad\text{and}\quad r=2m, \\ \theta(\eta)=\frac{T-T_\infty}{T_w-T_\infty},M=\frac{\sigma_f B_0^2}{a\rho_f},A_1=\frac{\mu_{hnf}}{\mu_f},\ u=\partial\psi/\partial y\text{ and }Ec=\frac{a^2}{AC_{p_f}}, \\ \varepsilon=\frac{c}{a},\qquad \delta=\lambda_0\sqrt{a\nu_f},Pr=\frac{(\mu C_p)_f}{k_f}, \end{gathered}\right\} \tag{14}$$

The thermo fluidic quantities of engineering interest in this study are the skin friction coefficient C_{fx} and the Nusselt number Nu_x[36]:

$$C_{fx}=\frac{\tau_w(x)}{\rho_f u_e^2},\qquad Nu_x=\frac{xq_w(x)}{k_f(T_w-T_\infty)}, \tag{15}$$

Eq. 15 can be expressed as

$$\mathrm{Re}_x^{1/2}C_f = \frac{\mu_{hnf}}{\mu_f}f''(0), \qquad \mathrm{Re}_x^{-1/2}\mathrm{Nu}_x = -\frac{k_{hnf}}{k_f}\theta'(0) \tag{16}$$

3. Numerical Solution

*3.1.*Application of weighted residual method

A detailed explanation of the technique can be found in[37, 38]. The following trial solutions for $f(\eta)$, and$\theta(\eta)$,are employed to solve the equations of velocity and energy equation.

$$f'(\eta) = \sum_{i=0}^{n} a_i\, e^{-\frac{i\eta}{3}}, \theta(\eta) = \sum_{k=1}^{n} b_k\, e^{-\frac{k\eta}{3}} \tag{17}$$

Subjected

$$f(0) = S, \quad f'(0) = \varepsilon + \delta\frac{A_1}{A_2}f''(0), \quad \theta(0) = 1, \\ f'(\eta) \longrightarrow 1, \theta(\eta) \longrightarrow 0 \text{as} \quad \eta \longrightarrow \infty, \tag{18}$$

At infinity, the boundary conditions are automatically satisfied. By replacing the trier functions, residual functions$R_f(a_i, b_l, c_l, \eta)$, and $R_\theta(a_i, c_l, \eta)$ for $i = 0 \cdots N$, $l = 1 \cdots N$ are obtained as:

$$\left.\begin{aligned} \int_0^{\infty} R_f e^{-\frac{i\eta}{3}} d\eta \approx \sum_{k=1}^{j}\left[A_k\left(e^{\eta}R_f e^{-\frac{i\eta}{3}}\right)_{\eta=x_k}\right] = 0 \\ \int_0^{\infty} R_\theta e^{-\frac{l\eta}{3}} d\eta \approx \sum_{k=1}^{j}\left[A_k\left(e^{\eta}R_\theta e^{-\frac{l\eta}{3}}\right)_{\eta=x_k}\right] = 0 \end{aligned}\right\} \tag{19}$$

The residual errors are kept to a minimum by the integration of the product of residues and weight functions $e^{-\frac{i\eta}{3}}$ with $i = 0,1,2, \ldots, N-2, l = 0,1,2, \ldots, N-2$ to zero. Figure 1 shows the graph of the residual functions $R(\eta)$. However, in the range of 0 to infinity, the residuals were reduced. Finally, the unknown coefficients were compute using MATHEMATICAL software. Figure 2 display the design of the numerical simulation plan.

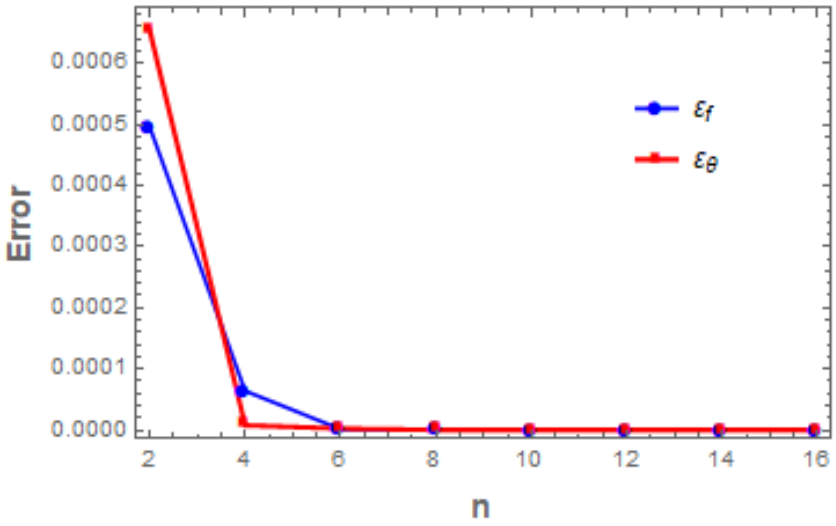


Fig. 1. Minimized residual error.

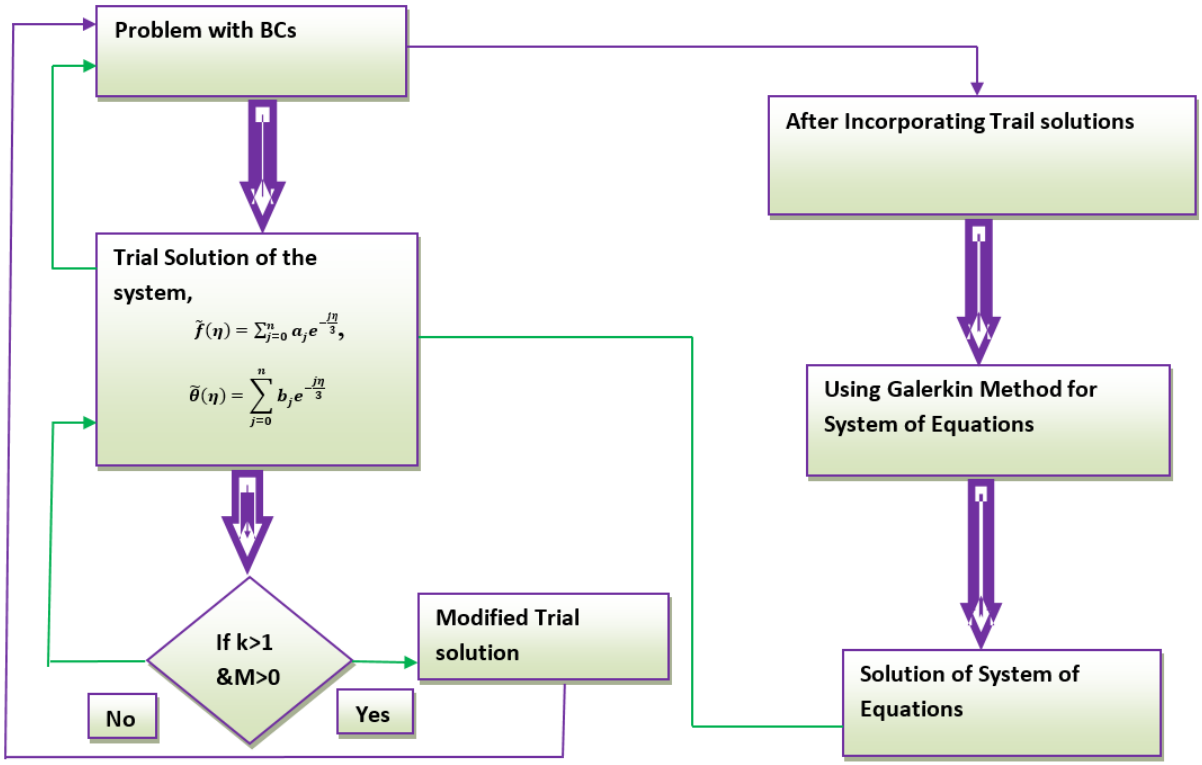


Fig. 2. The Galerkin Weighted Residual Method.

4. Results and Discussion

The purpose of this section is to investigate the physical significance of the numerical result for the hybrid nanosuspension in graphical form. The velocity flow f(η), fluid temperature θ(η), thermodynamic Irreversibility (Ns), Bejan number (Be) the skin friction($Re_x^{1/2}C_f$), and heat transfer rate($Re_x^{-1/2}Nu_x$) for $Cu - Fe_3O_4/H_2O$ hybrid nanofluid on non-linearly stretching permeable sheet has been numerically solve by GWRM. The variations of nanoparticle parameter on velocity flow, fluid temperature, and thermodynamic Irreversibility of the $Cu - Fe_3O_4/H_2O$ hybrid nanofluid are shown in Figure **3** (a-d). It is found in these figures that the higher of nanoparticle volume fraction reduce the fluid flow while abruptly upsurges the temperature in the entire domain. In general, this decrease in velocity has happened due to the recognized fact that the fluid is becoming more viscous when the effect of hybrid nanoparticles increases. Furthermore, As the hybrid nanofluid decreases in the stretching boundless domain, and the overall constituent volume mixes influence the reaction. Moreover, it was noticed that the momentum boundary layer increases the convective thermal transmission leading to an increase in the liquid bonding force. Therefore, the thermal and momentum boundary layer thicknesses increase also, the flow drags causes the fluid flow to be reduced due to higher of nanoparticle volume fraction. Substantially, increasing the volume fraction of nanoparticles improves thermal conductivity, which leads to an increase in the fluid temperature and thickness of the thermal boundary layer. As a result, the thermal border layer is improved to decrease heat diffusion, causing the system to increase temperature (Figure **3**b).The work of Colla et al. [39] has also reported on similar physical behavior in experiments. The $Cu - Fe_3O_4/H_2O$ hybrid nanofluid improves the performance of cooling and heating operations. The irreversibility magnitude and Bejan number rises as nanoparticle volume fraction varies. In both the entropy and the Bejan number profile, large elevations are noted due to their respective dominant with the Joule heating, fluid viscosity, and viscous dissipation as well as heat transfer near a permeable stretched sheet. Therefore, the irreversibility and irreversibility ratio diminish a small distance from the plate as the energy

dissipation gradually drops to the far stream. Consequently, as energy loss decreases, the entropy generation and the Bejan number for the hybrid nanofluid reactive mixture are minimized. Therefore, the volume fraction of the nanoparticles thereby minimizes the energy loss far away from the moving plate.

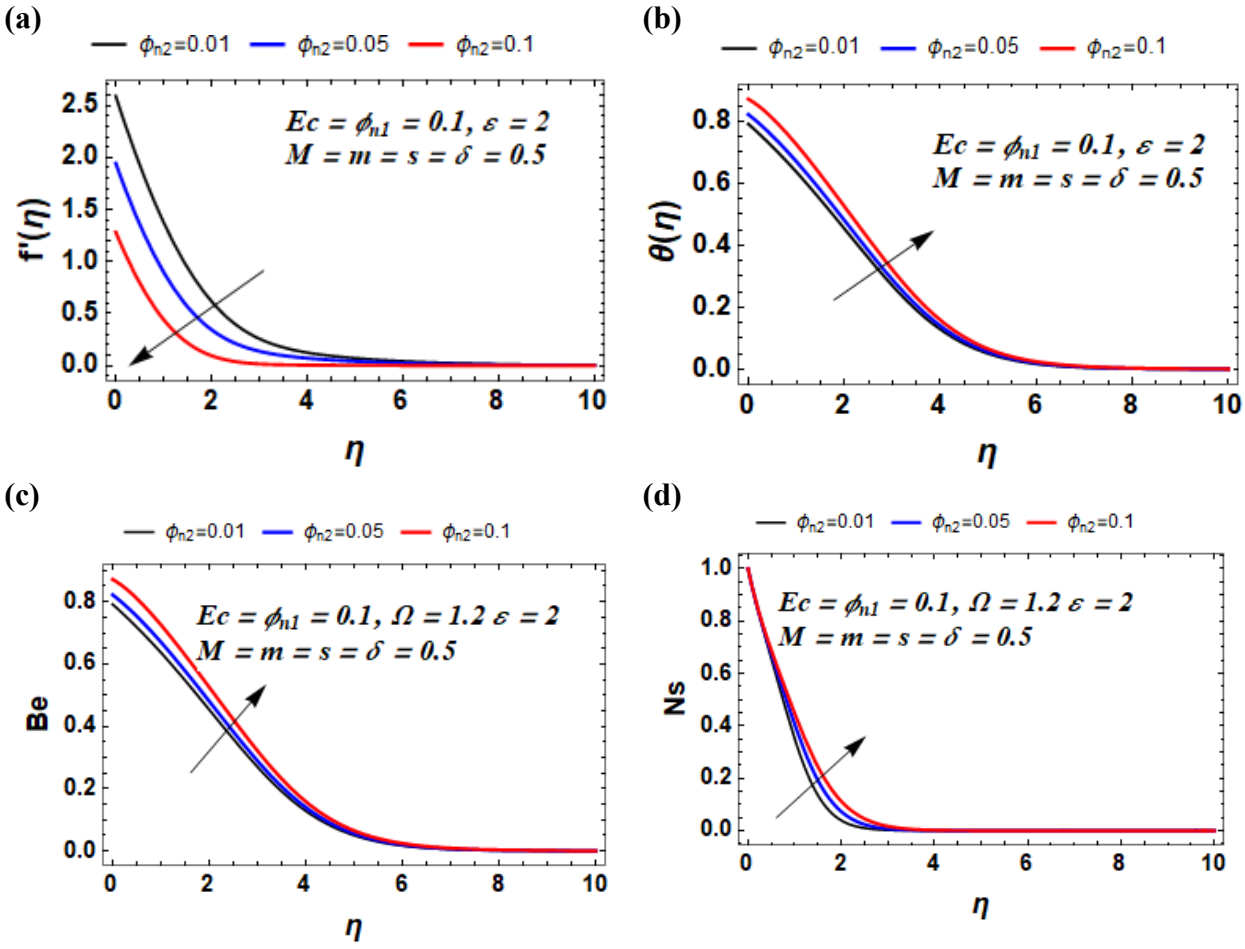


Fig. 3(a-d): Effect of nanoparticle volume fraction on (a) $f'(\eta)$, (b) $\theta(\eta)$, (c) Be, and (d) Ns.

Figure 4(a, b, c, and d) exemplify the percussion of the non-linearity m on the velocity flow, fluid temperature, thermodynamic Irreversibilities of the $Cu - Fe_3O_4/H_2O$ hybrid nanofluid. Consequently, the outcomes in both figures decrease significantly for the considered the $Cu - Fe_3O_4/H_2O$ mixture. This is because the nanoparticles produce low internal heat and conductivity, which leads to a retardation in reacting a mixture of velocity and heat transmission. Therefore. the stagnation hybrid nanofluid mixture decreases the non-linearity term. Conversely, near the permeable moving sheet in Figure 4 (c, and d), the non-linearity term causes an increment in entropy generation and Bejan number. Nevertheless, the entropy production and Bejan number are reduced due to limited heat dissipation and the loss of energy in the nano-liquid reactive mixture. Further, the irreversibility and Bejan number are continuously reduced in the free flow until no energy or heat is lost to the environment. Therefore, the hybrid nano liquid optimal efficiency is improved by a substantial reduction in the irreversible process. This is due to an increase in the nanoparticle's thermal conductivity strength. As a result, the irreversibility profile and ratio both decline.

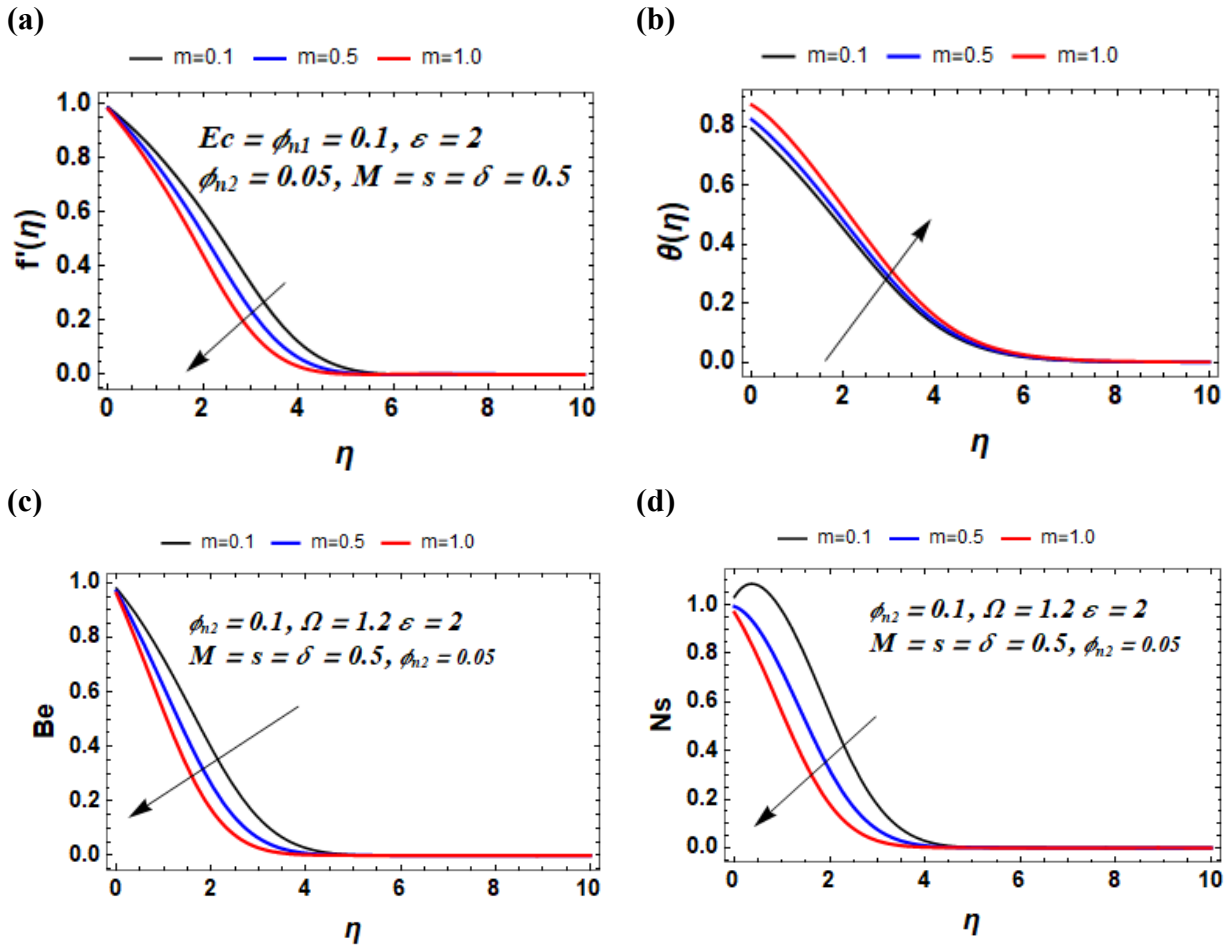


Fig. 4. (a-d): Effect of non-linearity term on (a) f′(η), (b) θ(η), and (c) Ns (d) Be.

The impact of the suction/injection parameter on the fluid flow, temperature profile, thermo-dynamic Irreversibilities are investigated in figure 5(a, b, c, d). The magnitude of the flow velocity and heat distribution reduce momentously for the considered $Cu - Fe_3O_4/H_2O$ hybrid mixture. However, the substantial declination is due to thinner momentum and heat boundary layers, which slowed the heat source terms and allowed more heat to escape the reactive mixture. Moreover, increased heat diffusion intensifies the hybrid nanoparticle bonding force, which causes the $Cu - Fe_3O_4/H_2O$ hybrid to drag. Therefore, the system reduces the reactive mixture flow rate. In addition, the increased heat loss in the environment reduces the heat volume in the vertically moving plate, as seen in figure 5d. hence, the temperature profile decreases. Figure 5 (c, and d)exhibit the absorption effect on the irreversibility of the hybrid nanofluid and the Bejan number. however, due to the dominance of nanofluid viscosity and viscous dissipation, a significant increase in irreversibility is observed. Also, the heat transfer rate for nanoparticles lowers due to a decrease in energy loss, which reduces entropy and the rate of irreversibility. Also, as the suction/injection term increases, the hybrid nanofluid entropy and the Bejan field are discouraged. Thus, the thermal conductivity of nanomaterials is boosted, and the effectiveness of the hybrid material blend is increased.

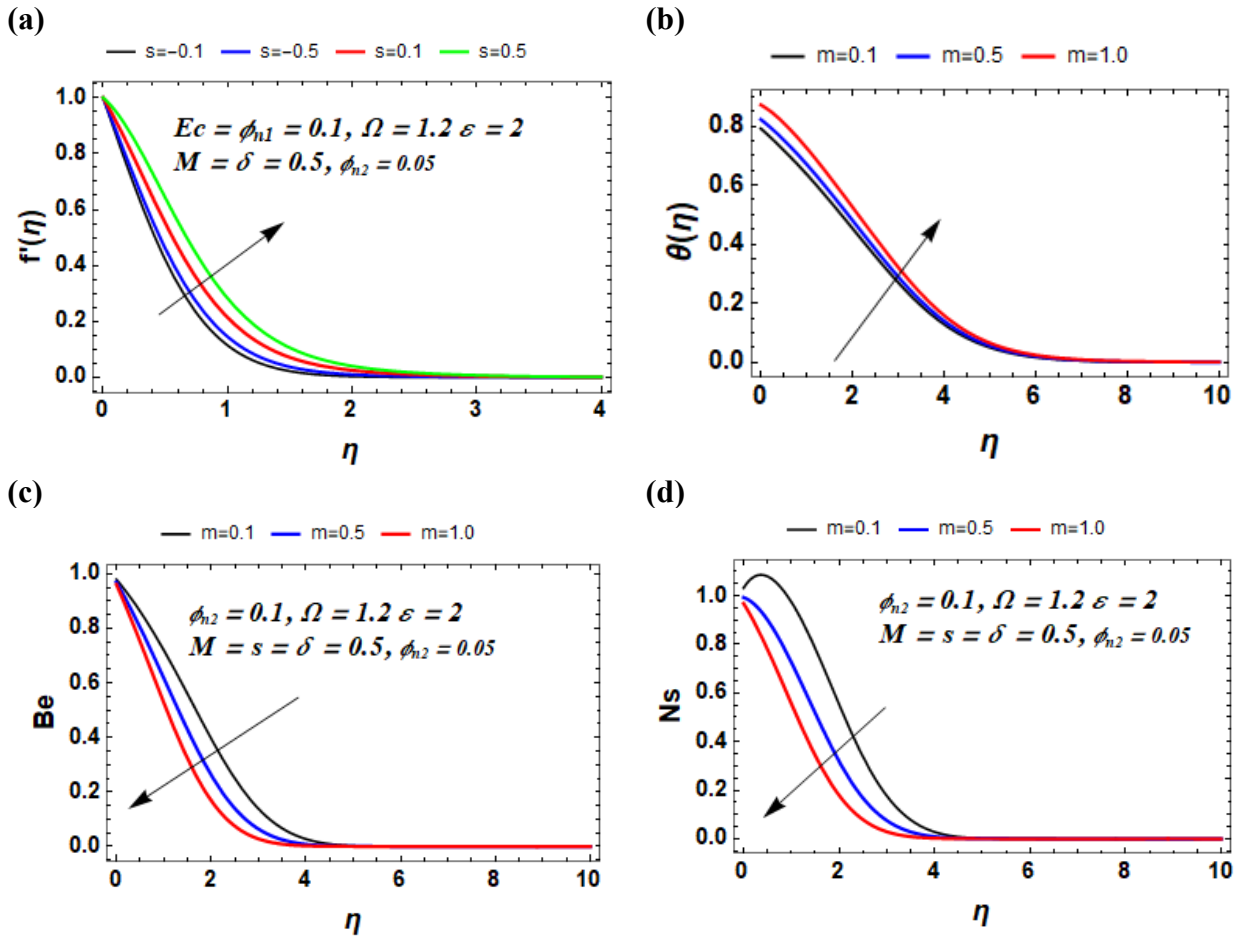


Fig. 5. (a-d) Effect of suction/injection parameter on (a) $f'(\eta)$, (b) θ(η), (c) Be, and (d) Ns.

Figure 6(a, b, and c) illustration the outcome of the velocity slip parameter (δ) on the velocity flow, fluid temperature, thermodynamic Irreversibilities of the $Cu - Fe_3O_4/H_2O$ hybrid nanofluid. Thus, the thermal conductivity of nanomaterials is boosted, and the effectiveness of the hybrid material blend is increased. As fluid particles are restrained from the free collision to nanofluid velocity distribution is thereby reduced (see Figure 6a). Also, the entropy generation and Bejan number profile for the reactive mixture is increased since the hybrid mixture has been regulated by heat transfer irreversibility. Consequently, the irreversible mixture of colloidal suspension diminishes to free flow before irreversibility disappears in the system as seen in Figure 6 (b and c). From Figure 6 (d) the Eckert number was shown to have an important influence on the temperature profile. Consequently, the association between enthalpy boundary layer difference and the considered nanofluid kinetic energy is known as the Eckert number, which is defined by dissipative heat transfer in a system. The Improvement of a chemical reaction term nano liquids increases the kinetic energy of nanoparticles steadily, which increases the collision rate of particles and so improves the distribution of temperature. The ratio of advective to heat-dissipation transport is therefore increasing, thereby increasing the heat transfer magnitude, which is why the temperature profile increases as seen Figure 6 (d). Figure 6e depicts the entropy generation and its ratio as irreversibility. Figure 6d shows that as the Eckert number is increased, the ratio of dissipated kinetic energy to transmitted thermal energy increases, resulting in a high irreversible rate in the $Cu - Fe_3O_4/H_2O$ hybrid nanofluidmixture. Also, the entropy production has risen, and the reactive combination is controlled by irreversibility due to a chemical reaction, as shown in Figure 6f. Increasing the dissipative term decreases the Bejan count since the mixing of hybrid nanofluid has been strengthened and the irreversibility of friction with thermal diminishes Therefore, the irreversibility of the thermodynamic transmission diminishes the Bejan profile and causes a general reduction (see Figure 6e).

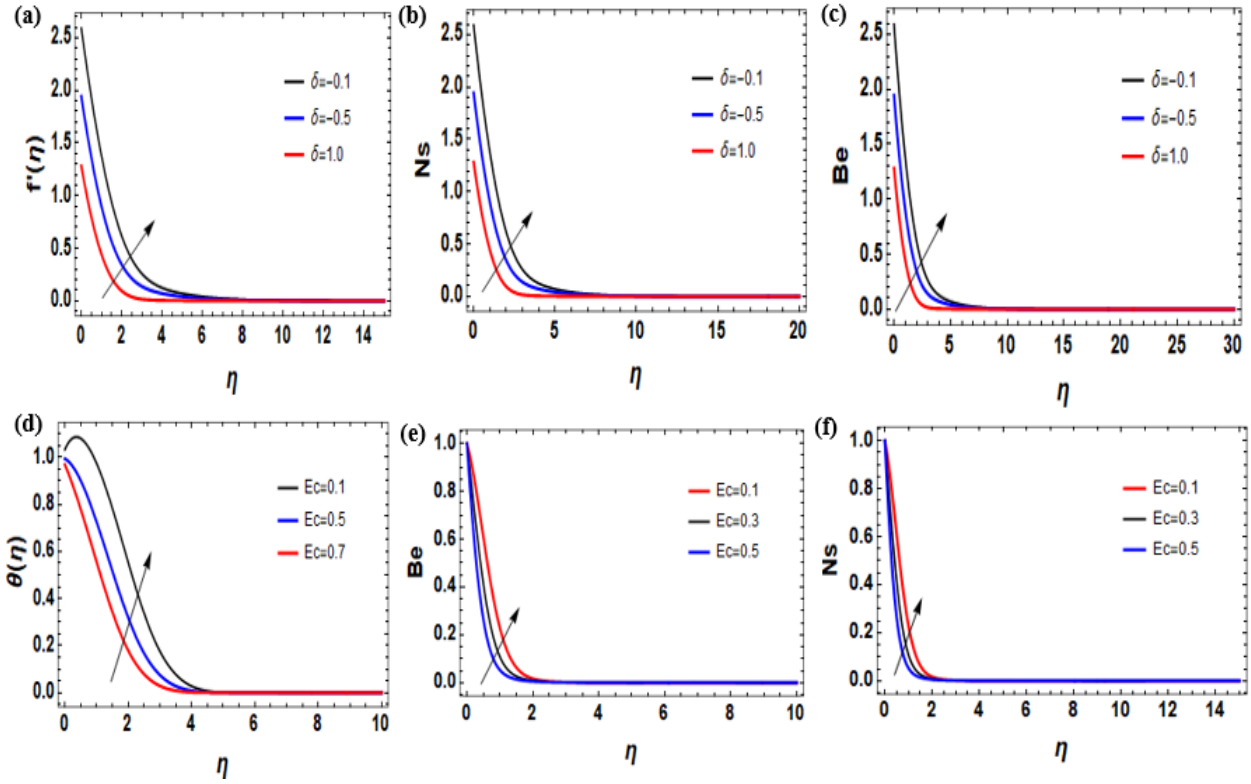


Fig. 6. (a-f) Effect of velocity slip parameter (δ) on (a) f′(η), (b) Ns, (c) Be, and Eckert number (Ec) on(d) θ(η),(e) Be, and (f) Ns.

The effect of magnetic field parameter (M) on velocity and temperature entropy generation and irreversibility ratio profiles of the $Cu - Fe_3O_4/H_2O$ hybrid nanofluid is elaborated in Figure 7 (a, b, c, and d). The figure also found that an increment in the magnetic field reduced the velocity flow. Physically, A magnetic field is occurred in an electrically conducting fluid and adds a retarding body force that transversally reacts in the path of the applied magnetics force. With the applied magnetics force, the magnetohydrodynamic drag force slows down the motion of the fluid. This outcome has an important impact on numerous industrial applications, for solidification procedures like casting and semiconductor applications for single crystal growth. These claims provide significant implications on quality control for the product when the liquids have solidification, the liquid flow, and turbulence exist in the solidifying fluid pool. In solidifying systems, the technique of magnetic fields has been used well to monitor melt convection. The mounting parameter of the magnetic field has a contrary impact on temperatures profile. The Lorentz heating servers a resistive nature to the system fluid flow. However, the Lorentz heating is used as an extra source of heat within the boundary layer. As the magnetic field value is increased in Figure 7c, heat transfer owing to viscous heating is accelerated all throughout the flow. However, energy lost to the surrounding vicinity of the permeable surface increases the magnitude of entropy generated because of irreversibility. For an increasing magnetic field term along the free stream, the irreversibility diminishes significantly as the heat discharge drops from the permeable surface. In figure 7d, the irreversibility ratio (Bejan number) due to heat transfer diminishes, which enhances the dominance of fluid viscosity and viscous heating. Therefore, the Bejan number profile reduces as the thermal boundary layer becomes thinner and causes more heat dissipation to the environment from the hybrid nanofluid mixture. Hence, the irreversibility ratio field is discouraged as presented in as heat diffuses out of the mixtures.

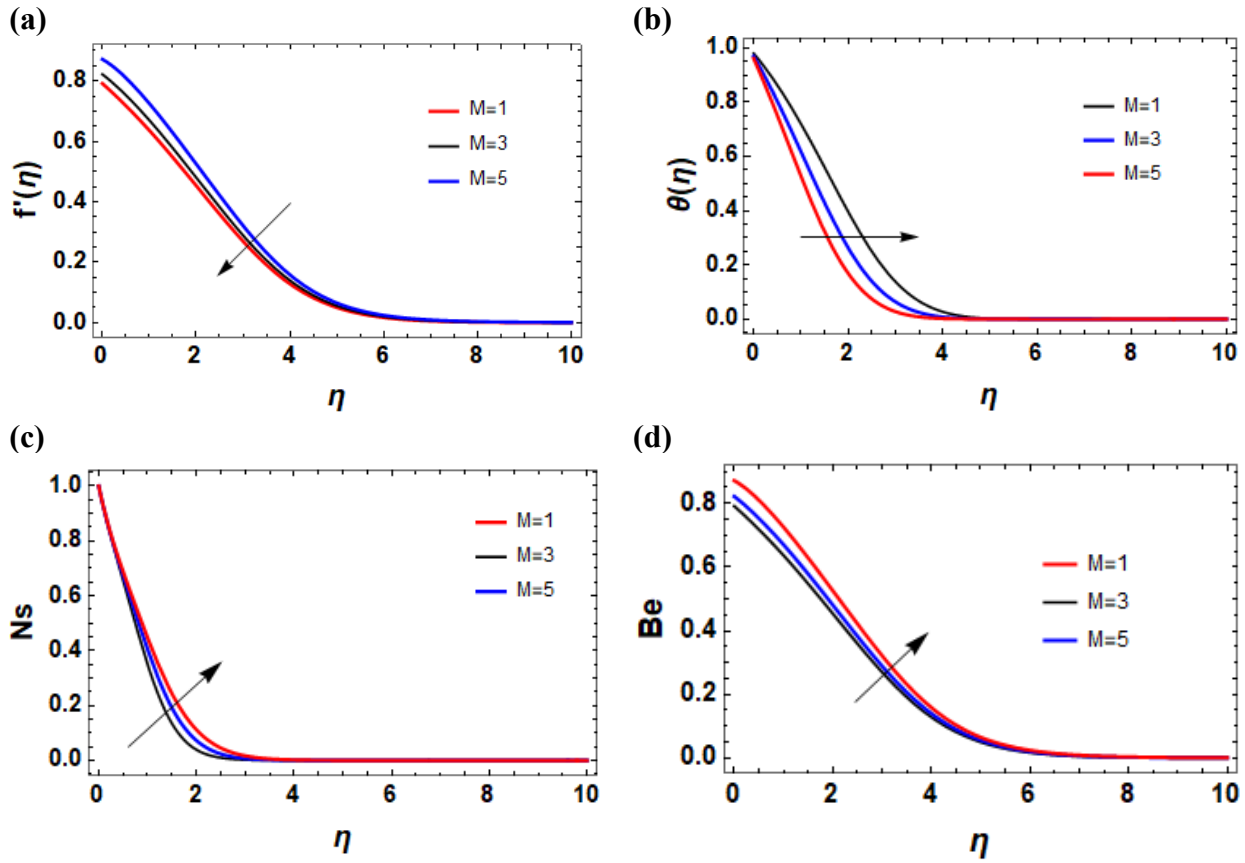


Fig. 7. (a-d) Effect of magnetic field parameter (M) on $(a)f'(\eta)$, (b)$\theta(\eta)$, (c)Ns, and (d)Be.

Table 2. GWRM solutions in different Convergence approximation orders when $M = Ec = S = \delta = 0.2$, $m = 1$, and $Pr = 6.2$

Number of iteration (N)	f′(η)	θ(η)
4	3.054620	0.233124
6	3.004633	0.180744
8	3.002122	0.98752
10	3.001933	0.987525
12	3.001933	0.98752
14	3.001933	0.180557
16	3.001933	0.180557
20	3.001933	0.180557
24	3.001933	0.180557
30	3.001933	0.180557

Table 3. Comparison of the skin friction with Lund et al. [40] and Liaquat et al. [21]

M	(φ_{Cu})	Present work	Lund et al. [40]	Liaquat et al. [21]
1	0.005	-1.3258	-1.325862	-1.3258
	002	-1.4046	-1.404648	-1.4046
	0.04	-1.5112	-1.511257	-1.5112
	0.06	-1.6201	-1.620177	-1.6201
1.5	0.02	-1.4911	-1.491175	-1.4911
	0.04	-1.6043	-1.604352	-1.6043
2.5	0.02	-1.5850	-1.585037	-1.5850
	0.04	1.7053	1.7053327	1.7053

Table 4. Values of velocity, temperature, skin friction coefficient C_{fx} and the Nusselt number Nu_x at the surface at $\varphi_{Cu-Fe_3O_4}$=0.1, Pr=6.2, $\delta = 0.5$

			(Cu-H_2O) nanofluid				(Fe_3O_4-H_2O) nanofluid			
M	ε	M	f(η)	θ(η)	$Re_x^{1/2}C_f$	$Re_x^{-1/2}Nu_x$	f(η)	θ(η)	$Re_x^{1/2}C_f$	$Re_x^{-1/2}Nu_x$
		0	2.11388	5.73467	0.00711	5245.51	2.24253	5.56432	0.00812	5256.29
	0.5	1	2.34655	5.62678	0.00895	5266.92	2.57643	5.54677	0.00955	5245.75
		2	2.55119	5.69567	0.00899	5281.67	2.78654	5.52244	0.01056	5222.33
0		0	0.90468	0.88755	0.00222	7742.72	0.83325	0.83468	0.00324	792.01
	-0.5	1	1.06652	0.81467	0.00256	7543.13	1.07577	0.80245	0.00324	754.96
		2	1.27214	0.73842	0.00389	7247.34	1.27652	0.77876	0.00465	735.52
		0	2.26679	5.78531	0.00711	5324.95	2.49864	5.63133	0.00813	5346.76
	0.5	1	2.54577	5.73972	0.00855	5367.43	2.69743	5.61876	0.00955	5233.57
0.2		2	2.77893	5.71665	0.00881	5390.03	2.89843	5.59234	0.01023	5289.53
		0	0.97356	0.97951	0.00234	9151.54	0.92356	0.97876	0.00323	919.65
	-0.5	1	1.13457	0.90873	0.00369	8876.83	1.19753	0.95123	0.00445	834.65
		2	1.34683	0.90934	0.00380	8654.21	1.37971	0.92876	0.00482	811.42

Table 5. Values of velocity, temperature, skin friction coefficient C_{fx} and the Nusselt number Nu_x at the surface at Pr=6.2, $\delta = 0.5$, m=0.1

			(Cu-H_2O) nanofluid				(Fe_3O_4-H_2O) nanofluid			
δ	ε	$\varphi_{Cu-Fe_3O_4}$	f(η)	θ(η)	$Re_x^{1/2}C_f$	$Re_x^{-1/2}Nu_x$	f(η)	θ(η)	$Re_x^{1/2}C_f$	$Re_x^{-1/2}Nu_x$
		0	2.1652	7.3461	0.00543	5124.66	2.15655	7.44564	0.00543	5124.77
	-0.5	0.1	2.4736	5.6342	0.00843	5245.136	2.60455	5.53556	0.00845	5122.31
0.5		0.2	2.5456	4.3562	0.01256	5368.97	2.70456	4.24545	0.01455	5111.44
		0	1.1724	0.8753	0.00235	643.28	1.18565	0.94353	0.00324	643.23
	0.5	0.1	1.1268	0.7654	1.35674	836.17	1.10456	0.82453	0.00424	812.87
		0.2	1.0245	0.5632	0.00467	1024.78	1.03456	0.85643	0.00554	1053.88
		0	2.3135	7.3568	0.00543	5156.60	2.35643	7.43453	0.00664	5124.77
	0.5	0.1	2.6075	5.4675	0.00876	5287.67	2.7564	5.54536	0.01002	5121.25
1		0.2	2.6578	4.2462	0.01235	5367.53	2.85664	4.26765	0.01354	5111.48
		0	1.3135	0.7435	0.00246	632.74	1.33563	0.93564	0.00386	654.74
	0.5	0.1	1.2367	0.6543	0.00386	817.12	1.24565	0.84567	0.00435	855.84
		0.2	1.1754	0.6346	0.00432	1024.44	1.18454	0.84675	0.00564	1001.33

Table 3 compares the outcome of $Re_x^{1/2}C_f$ for Cu-/water hybrid nanofluid for different values of φ_{Cu} when $\varphi_A = 0.1, m = M = Ec = S = \varepsilon = \delta = 0$, and $Pr = 6.135$ with the outcomes of the present work. However, present results agree with the precious results. Table 4 shows how the surface dimensionless velocity values increase with the transformation of the nanoparticles from Cu to Fe_3O_4. But at dimensionless temperature the reverse effect occurs. In addition, Cu -nanofluid has a greater

heat transfer rate from the surface than Fe_3O_4 nanofluid. This implies that cooling with Cu -nanofluid is better for surface hardness and strength. Table 5 show that, for Cu to Fe_3O_4 Nanoparticles, the surface velocity gradient values steadily increase by increasing the nanoparticle volume fraction from 10 to 20%. However, the dimensionless temperature drops by raising it for all types of nanoparticles. it was observed that the nanoparticles in the base fluid improved with increasing the heat transfer rate and the skin friction coefficient. As a result, the nanofluid of 20% nanoparticles is more active on mechanical properties than the nanofluid containing 10% nanoparticles. generally, the use of nanofluid to enhance the mechanical characteristics of the surface is better during the cooling process, this means that nanofluid is being used to boost the heat transfer rate by 10 to 40% than the pure H_20, resulting in an accelerated surface cooling that improves surface strength.

5. Conclusions

This study examined the heat transfer characteristics, and thermodynamic Irreversibility analysis of a two-dimensional non-linearly stretched permeable sheet with velocity slip and pre-scribed surface heat flux conveying water-based hybrid nanofluid induced by Joule heating and viscous dissipation effects. The following are the findings of this study:

1. The flow and thermal distributions reduce as the nonlinearity parameter improves.
2. An increase in Eckert number and magnetic field arises as the temperature of a fluid increases.
3. The slip parameter has a significant impact on skin friction, but the nonlinearity parameter has the opposite effect.
4. With a larger value of the velocity slip parameter, the flow is reduced.
5. The mounting values of the magnetic field, Eckert number, and suction/injection parameter improve the entropy generation while the nonlinearity parameter has an opposite impact.
6. The Bejan number profile is reduced by improving the magnetic field strength, Eckert number, suction/injection parameter, nonlinearity, while a contrary effect is found for the nanoparticle volume fraction.

References

[1] M. T. Kartal, The role of consumption of energy, fossil sources, nuclear energy, and renewable energy on environmental degradation in top-five carbon producing countries, Renewable Energy. 184 (2022) 871-880.

[2] B. Buonomo, A. Di Pasqua, O. Manca, S. Nappo, and S. Nardini, Entropy generation analysis of laminar forced convection with nanofluids at pore length scale in porous structures with Kelvin cells, International Communications in Heat Mass Transfer. 132 (2022) 105883.

[3] B. Moshfegh and M. Sandberg, Flow and heat transfer in the air gap behind photovoltaic panels, J. Sol. Energy Eng. 2 (1998) 287-301.

[4] A. M. Obalalu, A. O. Ajala, A. O. Akindele, O. A. Oladapo, O. O. Akintayo, and O. M. Jimoh, Computational study of magneto-convective non-Newtonian nanofluid slip flow over a stretching/shrinking sheet embedded in a porous medium, Computers Mathematics with Applications. 4 (2022) 123-128.

[5] J. A. Eastman, S. Choi, S. Li, W. Yu, and L. Thompson, Anomalously increased effective thermal conductivities of ethylene glycol-based nanofluids containing copper nanoparticles, Applied physics letters. 78 (2001) 718-720.

[6] F. Shahzad, W. Jamshed, S. U. D. Sathyanarayanan, A. Aissa, P. Madheshwaran, and A. Mourad, Thermal analysis on Darcy-Forchheimer swirling Casson hybrid nanofluid flow inside parallel plates in parabolic trough solar collector: An application to solar aircraft, International Journal of Energy Research. 45 (2021) 20812-20834.

[7] M. I. Hassan, I. A. Alzarooni, and Y. Shatilla, The effect of water-based nanofluid incorporating Al2O3 nanoparticles on heat pipe performance, Energy Procedia. 75 (2015) 3201-3206.

[8] F. Wang, M. I. Asjad, M. Zahid, A. Iqbal, H. Ahmad, and M. Alsulami, Unsteady thermal transport flow of Casson nanofluids with generalized Mittag–Leffler kernel of Prabhakar's type, Journal of materials research technology. 14 (2021) 1292-1300.

[9] S. Abdo and H. J. S. E. Saidani-Scott, Effect of using saturated hydrogel beads with alumina water-based nanofluid for cooling solar panels: Experimental study with economic analysis, 217 (2021) 155-164.

[10] S. A. Devi and S. S. U. Devi, Numerical investigation of hydromagnetic hybrid Cu–Al2O3/water nanofluid flow over a permeable stretching sheet with suction, International Journal of Nonlinear Sciences Numerical Simulation. 17 (2016) 249-257.

[11] A. R. Sajadi, S. S. Sadati, M. Nourimotlagh, O. Pakbaz, D. Ashtiani, and F. Kowsari, Experimental study on turbulent convective heat transfer, pressure drop, and thermal performance characterization of ZnO/water nanofluid flow in a circular tube, Thermal Science. 18 (2014) 1315-1326.

[12] M. Sheikholeslami, M. G. Bandpy, R. Ellahi, M. Hassan, S. Soleimani, and M. Materials, Effects of MHD on Cu–water nanofluid flow and heat transfer by means of CVFEM, Journal of Magnetism. 349 (2014) 188-200.

[13] U. Khan, A. Zaib, A. Ishak, and S. Bakar, Time-dependent Blasius–Rayleigh–Stokes flow conveying hybrid nanofluid and heat transfer induced by non-fourier heat flux and transitive magnetic field, Case Studies in Thermal Engineering. (2021) 101151.

[14] M. Slimane, Free vibration analysis of composite material plates" Case of a typical functionally graded FG plates ceramic/metal" with porosities, Nano Hybrids Composites. 25 (2019) 69-83.

[15] N. K. Konada, K. Suman, R. Bammidi, and B. A. Kumar, Investigation on Mechanical, Thermal and Bonding Properties of MWCNTs Reinforced Aramid/Epoxy Composite, Nano Hybrids and Composites. 30 (2020) 27-40.

[16] T. A. Yusuf and J. A. Gbadeyan, Entropy generation on maxwell fluid flow past an inclined stretching plate with slip and convective surface conditon: Darcy-forchheimer model, Nano Hybrids Composites. 26 (2019) 62-83.

[17] S. M. Hussain, W. Jamshed, V. Kumar, V. Kumar, K. S. Nisar, M. R. Eid, R. Safdar, A.-H. Abdel-Aty, and I. Yahia, Computational analysis of thermal energy distribution of electromagnetic Casson nanofluid across stretched sheet: Shape factor effectiveness of solid-particles, Energy Reports. 7 (2021) 7460-7477.

[18] S. Suresh, K. Venkitaraj, P. Selvakumar, and M. Chandrasekar, Synthesis of Al2O3–Cu/water hybrid nanofluids using two step method and its thermo physical properties, Colloids Surfaces A: Physicochemical Engineering Aspects. 388 (2011) 41-48.

[19] M.R. Khan, A.S. Al-Johani, A.M. Elsiddieg, T. Saeed, and A.M. Abd Allah, The computational study of heat transfer and friction drag in an unsteady MHD radiated Casson

fluid flow across a stretching/shrinking surface, International Communications in Heat Mass Transfer. 130 (2022) 105832.

[20] R. Turcu, A. Darabont, A. Nan, N. Aldea, D. Macovei, D. Bica, L. Vekas, O. Pana, M. Soran, and A. Koos, New polypyrrole-multiwall carbon nanotubes hybrid materials, Journal of optoelectronics dvanced materials. 8 (2006) 643-647.

[21] L. A. Lund, Z. Omar, J. Raza, and I. Khan, Magnetohydrodynamic flow of Cu–Fe 3 O 4/H 2 O hybrid nanofluid with effect of viscous dissipation: Dual similarity solutions, Journal of Thermal Analysis Calorimetry. 143 (2021) 915-927.

[22] N. Acharya, S. Maity, and P. K. Kundu, Influence of inclined magnetic field on the flow of condensed nanomaterial over a slippery surface: the hybrid visualization, Applied Nanoscience. 10 (2020) 633-647.

[23] A. M. Obalalu, Heat and mass transfer in an unsteady squeezed Casson fluid flow with novel thermophysical properties: Analytical and numerical solution, Heat Transfer. 50 (2021) 7988-8011.

[24] S. Manjunatha and B. Gireesha, Effects of variable viscosity and thermal conductivity on MHD flow and heat transfer of a dusty fluid, Ain Shams Engineering Journal. 7 (2016) 505-515.

[25] O.D. Makinde and A.S. Eegunjobi, Entropy Analysis of Thermally Radiating Magnetohydrodynamic Slip Flow of Casson Fluid in a Microchannel Filled with Saturated Porous Media, Journal of Porous Media. 19 (2016) 799-810.

[26] M. Hassan, S. Ali, W. Aich, F. Khlissa, B. Ayadi, and L. Kolsi, Transport pattern of Non-Newtonian mass and thermal energy under two diverse flow conditions by using modified models for thermodynamics properties, Case Studies in Thermal Engineering. 29 (2022) 101714.

[27] P. Vyas and S. J. J. R. a. O. P. S. Soni, Entropy analysis for MHD Casson fluid flow in a channel subjected to weakly temperature dependent convection coefficient and hydrodynamic slip, Rajasthan Academy of Physical Sciences. 15 (2016) 1-18.

[28] M. H. Abolbashari, N. Freidoonimehr, F. Nazari, and M. M. Rashidi, Analytical modeling of entropy generation for Casson nano-fluid flow induced by a stretching surface, J Advanced Powder Technology. 26 (2015) 542-552.

[29] R.K. Tiwari, M.K.J.I.J.O. H. Das, and M. Transfer, Heat transfer augmentation in a two-sided lid-driven differentially heated square cavity utilizing nanofluids, 50 (2007) 2002-2018.

[30] M. Ouni, L.M. Ladhar, M. Omri, W. Jamshed, and M.R. Eid, Solar water-pump thermal analysis utilizing copper–gold/engine oil hybrid nanofluid flowing in parabolic trough solar collector: Thermal case study, Case Studies in Thermal Engineering. 30 (2022) 101756.

[31] W. Ibrahim, Magnetohydrodynamics (MHD) flow of a tangent hyperbolic fluid with nanoparticles past a stretching sheet with second order slip and convective boundary condition, Results in physics. 7 (2017) 3723-3731.

[32] W. Jamshed, N. a. a. M. Nasir, S.S.P.M. Isa, R. Safdar, F. Shahzad, K.S. Nisar, M.R. Eid, A.-H. Abdel-Aty, and I. Yahia, Thermal growth in solar water pump using Prandtl–Eyring hybrid nanofluid: a solar energy application, Scientific reports. 11 (2021) 1-21.

[33] J. Mustafa, S. Alqaed, and M. Sharifpur, Numerical study on performance of double-fluid parabolic trough solar collector occupied with hybrid non-Newtonian nanofluids: Investigation of effects of helical absorber tube using deep learning, Engineering Analysis with Boundary Elements. 140 (2022) 562-580.

[34] W. Ashraf, H. Junaid Anjum, and I. Khan, Energy Transformation and Entropy Investigation in the Nanofluid Composed by γ-Nanomaterial over a Permeable Convective Surface with Solar Thermal Radiation: Numerical Analysis, Frontiers in Energy Research. 507.

[35] S. Bellout and R. Bessaïh, Mixed convection and entropy production of a hybrid nanofluid in a porous cylindrical enclosure with rotating top wall, Heat Transfer. 51 (2022) 3540-3561.

[36] A.M. Obalalu, "Heat Generation Fluid of Forced Convective Flow through a Channel with Permeable Walls and Suction/Injection," Kwara State University (Nigeria), 2019.

[37] A.M. Obalalu, I. Kazeem, A. Abdulrazaq, O.A. Ajala, A. Oluwaseyi, A.T. Adeosun, L.L. Adebayo, and F. A. Wahaab, Numerical simulation of entropy generation for casson fluid flow through permeable walls and convective heating with thermal radiation effect, Journal of the Serbian Society for Computational Mechanics. 14 (2020) 503-519.

[38] A.M. Obalalu, Performance of Variable Electrical Field (VEF) on Casson Flow Through an Inclined Annular Micro-Channel Embedded in a Porous Medium: Numerical Solution by Using Spectral Collocation Method, Petroleum Coal. 63 (2021).

[39] L. Colla, L. Fedele, M. Scattolini, and S. Bobbo, Water-based Fe2O3 nanofluid characterization: thermal conductivity and viscosity measurements and correlation, Advances in Mechanical Engineering. 4 (2012) 674947.

[40] L.A. Lund, Z. Omar, I. Khan, A.H. Seikh, E.-S. M. Sherif, K.S.J.J.O.M.R. Nisar, and Technology, Stability analysis and multiple solution of Cu–Al2O3/H2O nanofluid contains hybrid nanomaterials over a shrinking surface in the presence of viscous dissipation, 9 (2020) 421-432.